

## Supplementary Information

### Kinetics and Mechanism Effects of 2D Carbon Supports in Hydrogen Spillover Composites

Lu Han <sup>\*a</sup>, Pengfei Song<sup>a</sup>, Rui Zhang<sup>b</sup>, Liuyan Zhu<sup>a</sup>, Sibo Shen<sup>a</sup>, Lijiang Wang<sup>a</sup>, Xingxing

Shen<sup>a</sup>

<sup>a</sup> College of Chemical Engineering, Hebei Normal University of Science and Technology,

Qinhuangdao, Hebei 066004, China. E-mail: hl3395@hevttc.edu.cn

<sup>b</sup> College of Horticultural Science & Technology, Hebei Normal University of Science and

Technology, Qinhuangdao, Hebei 066004, China.

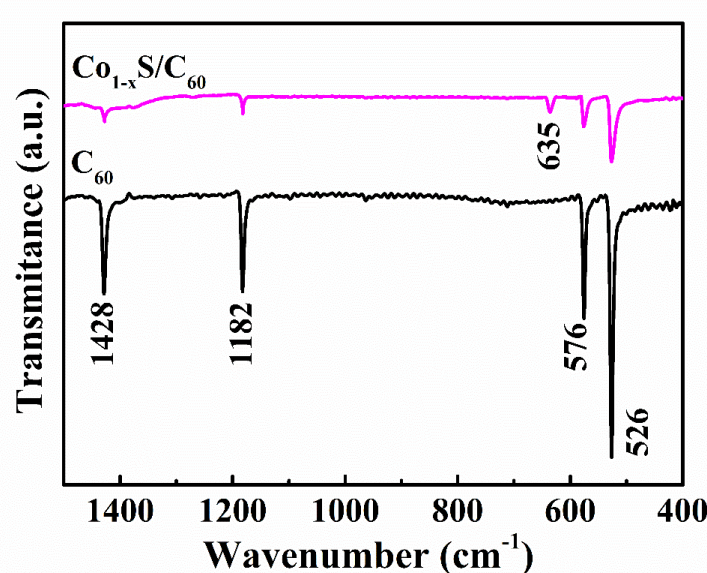


Fig. S1 Raman spectra of the raw  $\text{C}_{60}$  and  $\text{Co}_{1-x}\text{S}/\text{C}_{60}$  composites.

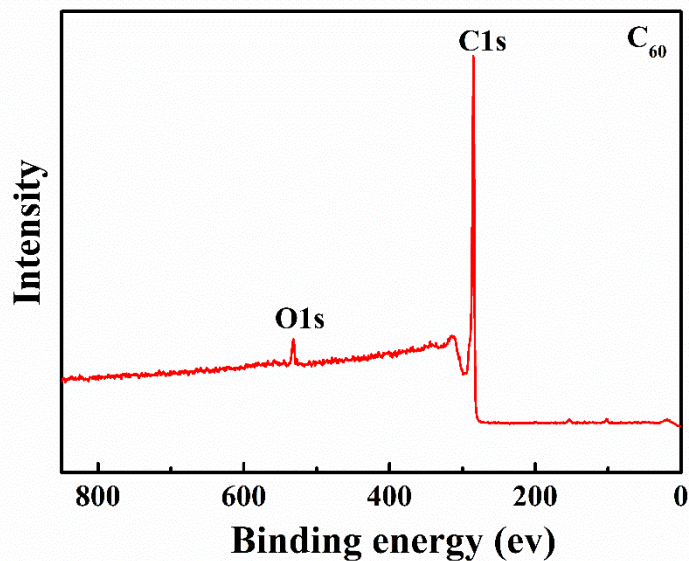


Fig. S2 XPS spectrum of the raw C<sub>60</sub>.

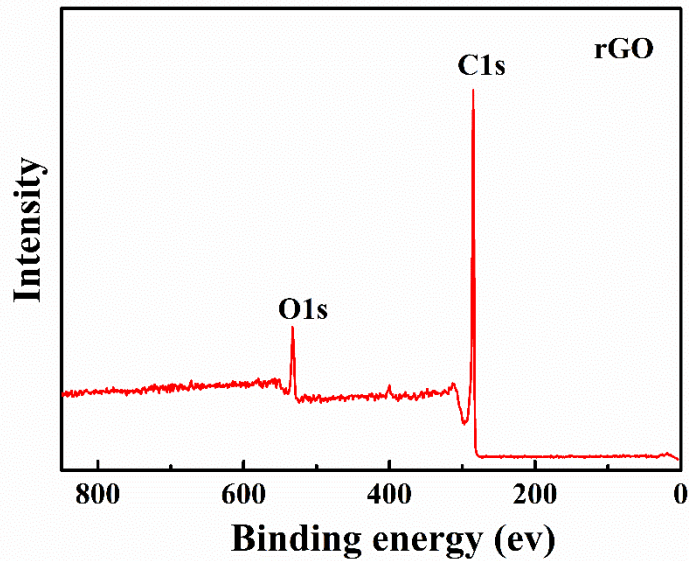


Fig. S3 XPS spectrum of the raw rGO.

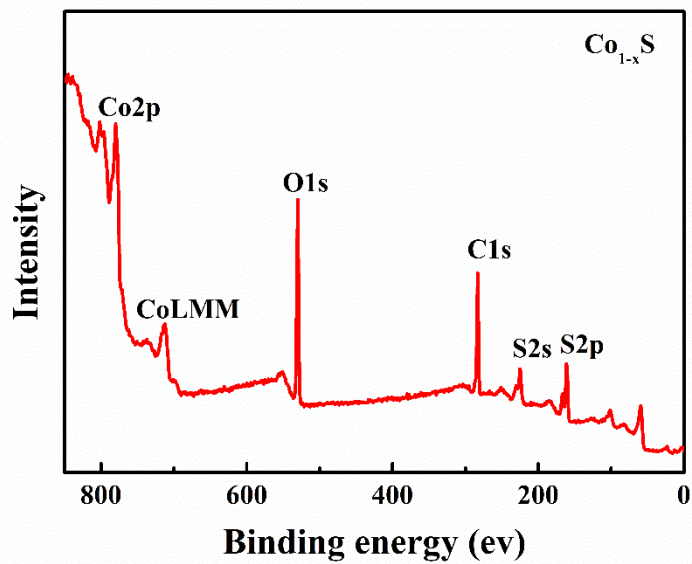


Fig. S4 XPS spectrum of the  $\text{Co}_{1-x}\text{S}$ .

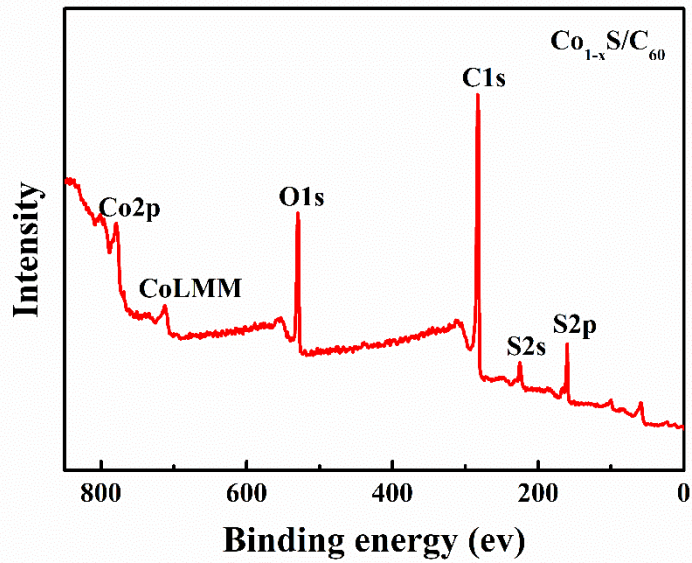


Fig. S5 XPS spectrum of the  $\text{Co}_{1-x}\text{S}/\text{C}_{60}$  composites.

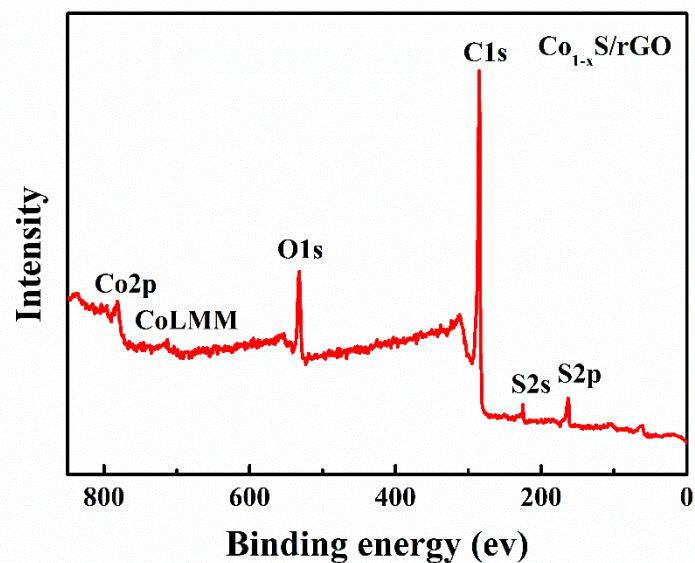


Fig. S6 XPS spectrum of the  $\text{Co}_{1-x}\text{S}/\text{rGO}$  composites.

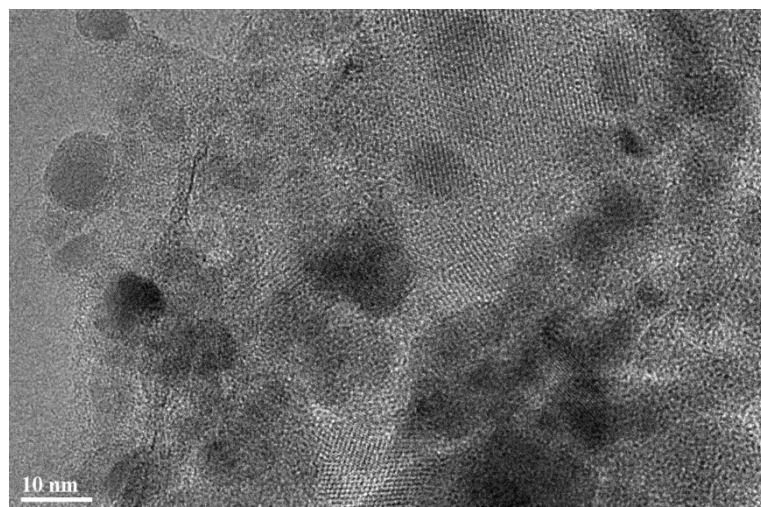


Fig. S7 HRTEM images of the  $\text{Co}_{1-x}\text{S}/\text{C}_{60}$  composites.

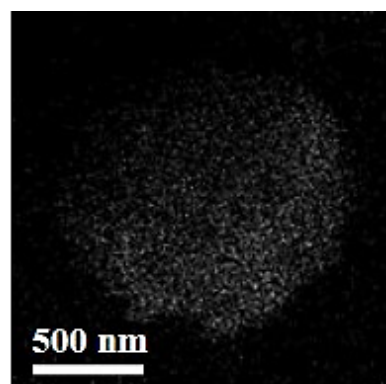


Fig. S8 EDS elemental mapping images of C in the  $\text{Co}_{1-x}\text{S}/\text{C}_{60}$  composites.

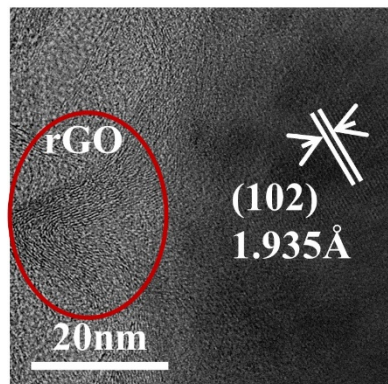


Fig. S9 HRTEM images of the  $\text{Co}_{1-x}\text{S}/\text{rGO}$  composites.

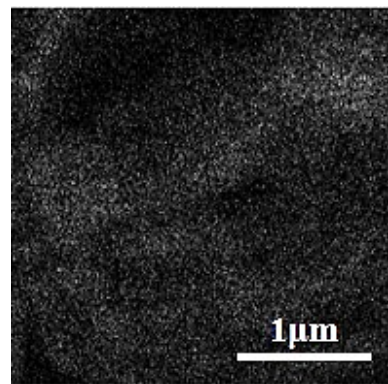


Fig. S10 EDS elemental mapping images of C in the  $\text{Co}_{1-x}\text{S}/\text{rGO}$  composites.

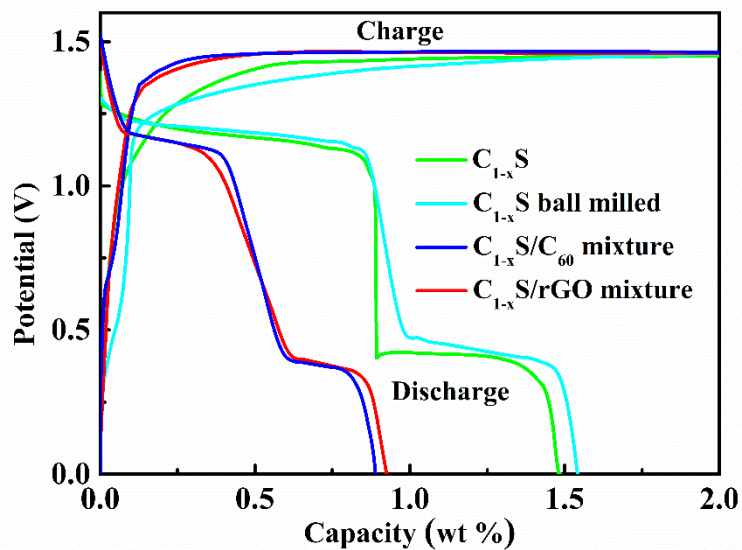


Fig. S11 Charge-discharge curves of the  $\text{Co}_{1-x}\text{S}$  and  $\text{Co}_{1-x}\text{S}$  ball milled for 10 h and  $\text{Co}_{1-x}\text{S}/\text{C}_{60}$  and  $\text{Co}_{1-x}\text{S}/\text{rGO}$  mixtures.

Tab. S1 Hydrogen storage capacity retention ratios of the different samples.

Sample	Hydrogen storage capacity (wt %)	Capacity (wt %)/Ratio (%)		
		I voltage plateaus	II voltage plateaus	III voltage plateaus
C <sub>60</sub>	0.50	—	—	—
rGO	0.31	—	—	—
Co <sub>1-x</sub> S	1.49	0.89/59	—	0.60/41
Co <sub>1-x</sub> S ball milled	1.54	0.99/64	—	0.55/36
Co <sub>1-x</sub> S/C <sub>60</sub> composites	4.36	0.78/18	2.57/59	1.00/23
Co <sub>1-x</sub> S/C <sub>60</sub> mixture	0.94	0.59/63	—	0.35/37
Co <sub>1-x</sub> S/rGO composites	5.02	0.50/10	2.71/54	1.81/36
Co <sub>1-x</sub> S/rGO mixture	1.00	0.63/63	—	0.37/37

Tab. S2 Comparison of hydrogen storage capacity with other reported materials.

No	Materials	Hydrogen Storage Capacities (wt %)	Reference
1	Pd/B-rGO	0.33 wt %	[1]
2	BaMoO <sub>4</sub> /ZnO-GO	0.79 wt %	[2]
3	Co <sub>9</sub> S <sub>8</sub> + CoRGO	2.38 wt %	[3]
4	Ni-ZrO <sub>2</sub> -rGO	1.54 wt %	[4]
5	C <sub>60</sub> /Co	3.32 wt %	[5]
6	C <sub>60</sub> /CoB	2.24 wt %	[6]
7	Pt-C <sub>60</sub>	1.6 wt %	[7]
8	Na <sub>6</sub> C <sub>60</sub>	2.1 wt %	[8]
9	Co <sub>1-x</sub> S/C <sub>60</sub> this work	4.36 wt %	----
10	C <sub>1-x</sub> S/rGO this work	5.02 wt %	----

Tab. S3 Hydrogen storage capacities of the different samples.

Sample	Hydrogen storage Capacity (wt %)	Capacity after 50 Cycles (wt %)	Capacity retention Ratio (%)
Co <sub>1-x</sub> S/rGO composites	5.02	4.41	88
Co <sub>1-x</sub> S/C <sub>60</sub> composites	4.36	3.48	80
Co <sub>1-x</sub> S composites	1.49	0.90	64
rGO	0.30	—	—
C <sub>60</sub>	0.50	—	—

Tab. S4 Comparison of CoS/C<sub>60</sub> and CoS/rGO hydrogen absorption systems.

Items	CoS/C <sub>60</sub>	CoS/rGO
H-H bond length for CoS-H <sub>2</sub>	0.78 Å	
Adsorption energy for CoS-H <sub>2</sub>	-6.9 kcal mol <sup>-1</sup>	
H-H bond length for one H <sub>2</sub> adsorption	0.79 Å	0.78 Å
C-Co bond length for one H <sub>2</sub> adsorption	1.82 Å	1.70 Å
Adsorption energy when one H <sub>2</sub> is adsorbed	-29.4 kcal mol <sup>-1</sup>	-15.5 kcal mol <sup>-1</sup>
H-H bond length when spillover occurs	0.79 Å	0.79 Å
C-Co bond length for one H <sub>2</sub> adsorption	1.70 Å	1.69 Å
Adsorption energy when spillover occurs	-30.7 kcal mol <sup>-1</sup>	-16.2 kcal mol <sup>-1</sup>
Specific surface area	C <sub>60</sub> : 33.6 m <sup>2</sup> g <sup>-1</sup>	rGO: 269.8 m <sup>2</sup> g <sup>-1</sup>

#### Quantum chemical computational details

All calculations in this work were performed using Gaussian 09 program package<sup>9</sup>. Full geometry optimizations were performed to locate all the stationary points, using the B3LYP method<sup>10</sup> with the 6-31++G\*\*<sup>11,12</sup> basis for S, C, H, and LANL2DZ for Co, namely B3LYP/6-31++G\*\*//LANL2DZ. Dispersion corrections were computed with Grimme's D3(BJ) method in optimization<sup>13</sup>. Harmonic vibrational frequency was performed at the same level to guarantee no imaginary frequency in the molecules, i.e., they locate on the minima of the potential energy surface. Convergence parameters of

the default threshold were retained (maximum force within  $4.5 \times 10^{-4}$  Hartrees/Bohr and root mean square (RMS) force within  $3.0 \times 10^{-4}$  Hartrees/Radian) to obtain the optimized structure. The optimal structure was identified, given that all calculations for structural optimization were successfully converged within the convergence threshold of no imaginary frequency during the process of vibration analysis.

Tab. S5 High rate discharge performances of the different electrodes.

Sample	HRD200	HRD400	HRD600	HRD800	HRD1000
Co <sub>1-x</sub> S/rGO Composites	93.2	89.3	84.7	82.1	80.4
Co <sub>1-x</sub> S/C <sub>60</sub> Composites	88.1	82.4	77.6	73.7	70.5

Tab. S6 Electrochemical kinetic parameters of different electrodes.

Sample	R <sub>p</sub> (mΩ)	i <sub>0</sub> (mA g <sup>-1</sup> )	D/r <sub>0</sub> <sup>2</sup> (10 <sup>-5</sup> cm <sup>2</sup> s <sup>-1</sup> )
Co <sub>1-x</sub> S/rGO Composites	363	70.69	6.92
Co <sub>1-x</sub> S/C <sub>60</sub> Composites	498	51.55	5.38

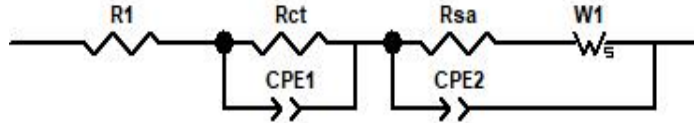


Fig. S12 Equivalent circuit of EIS of hydrogen storage electrodes.

Tab. S7 Component parameters of the equivalent circuit of EIS.

Sample	R <sub>1</sub> (Ω)	R <sub>ct</sub> (Ω)	R <sub>sa</sub> (Ω)
Co <sub>1-x</sub> S/rGO Composites	0.253	0.031	0.526
Co <sub>1-x</sub> S/C <sub>60</sub> Composites	0.294	0.052	0.740

## Reference

- 1 E. Boateng, J. S. Dondapati, A. R. Thiruppatti and A. Chen, International Journal of Hydrogen Energy, 2020, 45, 28951-28963.
- 2 F. Karkeh-Abadi, M. Ghiyasiyan-Arani and M. Salavati-Niasari, Ultrasonics Sonochemistry, 2022, 90, 106167.
- 3 H. Liu, W. Liu, P. Chen, J. Zhao and Z. Su, International Journal of Energy Research, 2020, 44, 11742-11755.
- 4 M. Kaur and K. Pal, Journal of Materials Science: Materials in Electronics, 2020, 31, 10903-10911.
- 5 D. Bao, P. Gao, X. D. Shen, C. Chang, L. Q. Wang, Y. Wang, Y. J. Chen, X. M. Zhou, S. C. Sun, G. B. Li and P. P. Yang, Acs Applied Materials & Interfaces, 2014, 6, 2902-2909.
- 6 L. Sha, P. Gao, X. Li and X. Bai, Journal of Organometallic Chemistry, 2018, 863, 90-94.
- 7 X. L. Wang and J. P. Tu, Applied Physics Letters, 2006, 89, 064101.
- 8 D. A. Knight, J. A. Teprovich, Jr., A. Summers, B. Peters, P. A. Ward, R. N. Compton and R. Zidan, Nanotechnology, 2013, 24, 455601.
- 9 R. A. Gaussian09, Inc., Wallingford CT, 2009, 121, 150-166.
- 10 R. Krishnan, J. S. Binkley, R. Seeger and J. A. Pople, The Journal of chemical physics, 1980, 72, 650-654.
- 11 F. Weigend and R. Ahlrichs, PCCP, 2005, 7, 3297-3305.
- 12 S. Xu, T. He, J. Li, Z. Huang and C. Hu, Applied Catalysis B: Environmental, 2021, 292, 120145.
- 13 S. Grimme, J. Antony, S. Ehrlich and H. Krieg, The Journal of chemical physics, 2010, 132, 154104.